CALIBRATION and PERFORMANCE MEASUREMENTS for the NASA DEEP SPACE NETWORK APERTURE ENHANCEMENT PROJECT (DAEP)

Remi C. LaBelle[a], David J. Rochblatt[a]

[a]Jet Propulsion Laboratory, California Institute of Technology, 4800 Oak Grove Drive, Pasadena, CA 91109, USA, remi.labelle@jpl.nasa.gov, david.rochblatt@jpl.nasa.gov

Abstract

The NASA Deep Space Network (DSN) has recently constructed two new 34-meter antennas at the Canberra Deep Space Communications Complex (CDSCC). These new antennas are part of the larger DAEP project to add six new 34-meter antennas to the DSN, including two in Madrid, three in Canberra and one in Goldstone (California). The DAEP project included development and implementation of several new technologies for the S, X, K~~a~~ (26 GHz) and Ka (32 GHz) -band uplink and downlink electronics, as previously reported. The electronics upgrades were driven by several different considerations, including parts obsolescence, cost reduction, improved reliability and maintainability, and capability to meet future performance requirements. The new antennas are required to support TT&C links for all of the NASA deep-space spacecraft, as well as for several international partners. Some of these missions, such as Voyager 1 and 2, have very limited link budgets, which results in demanding requirements for system G/T performance. These antennas are also required to support radio science missions with several spacecraft, which dictate some demanding requirements for spectral purity, amplitude stability and phase stability for both the uplink and downlink electronics. After completion of these upgrades, a comprehensive campaign of tests and measurements took place to characterize the electronics and calibrate the antennas. Radiometric measurement techniques were applied to characterize, calibrate, and optimize the performance of the antenna parameters. These included optical and RF high-resolution holographic and total power radiometry techniques. These techniques, which are described in the article, resulted in the highest antenna aperture efficiency in the DSN, of 66% achieved, at the highest operating frequency of the antenna, which is Ka-Band (32-GHz). The other measurements and results described include antenna noise temperature, photogrammetry and holography alignment of antenna panels, beam-waveguide mirrors, and subreflector, antenna aperture efficiencies and G/T versus frequency, and antenna pointing models.

The first antenna (DSS-35) was entered into operations in October, 2014 and the 2nd antenna (DSS-36) in October, 2016. This paper describes the measurement techniques and results of the testing and calibration for both antennas, along with the driving requirements.

Keywords: Telemetry tracking and command system, Deep space communication equipment, beam waveguide antenna, antenna calibration, antenna holography

1. Introduction

The Deep Space Network Aperture Enhancement Project (DAEP) was begun in 2010 to support NASA's current and future deep space tracking requirements [1]. The long-term goal of the project is to have four 34-meter beam waveguide (BWG) antennas at each of the DSN complexes, in Goldstone, California, Madrid, Spain and Canberra, Australia. The four combined (arrayed) BWG antennas will then have the equivalent receive sensitivity of the 70-meter antenna at each complex, if needed. In addition, the future addition of an 80 kW transmitter to any one 34-meter antenna will give it the equivalent effective isotropic radiated power (EIRP) of a 70-meter antenna with a 20 kW transmitter. The basic design of the BWG antennas is shown in Fig. 1.

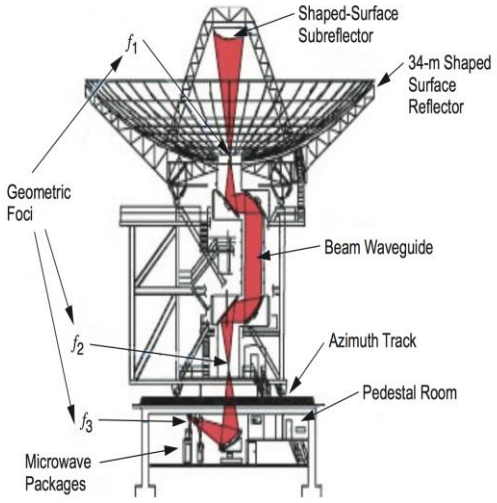

Fig. 1 A diagram of a DSN 34-meter BWG antenna, indicating the three foci at F1, F2 and F3.

The first two of six new 34-meter beam waveguide (BWG) antennas are now completed and operational, the first of which, in Canberra, is shown in Fig. 2. Various design upgrades were implemented in both the uplink and downlink electronics, as previously reported [2]. The electronics upgrades were driven by several different considerations, including parts obsolescence, cost reduction, improved reliability and maintainability, and capability to meet future performance requirements. After completion of the electronics installations for each antenna, a comprehensive campaign of tests was conducted, to characterize the electronics and calibrate the antennas. The antenna optimization included both optical and RF holographic techniques, resulting in the highest antenna aperture efficiency, at Ka-band, in the DSN (66%).

Fig. 2 The DSS-35 antenna in Canberra

2. Performance requirements

The "standard" frequencies for all BWG antennas in the DSN are X-band uplink (7145-7235 MHz) and X (8400-8500) and Ka-band (31800-32300 MHz) downlink. In addition, a second BWG antenna at each complex is planned to be equipped with S-band uplink (2025-2120 MHz) and downlink (2200-2300 MHz). The "standard" transmitter power for X-band is 20 kW, while the S-band antennas will have one antenna with 20 kW and one with 250 W. In addition, the X-band feeds that are being delivered under the DAEP project have the capability to be used at 80 kW in the future. However, at this point in time, only one antenna (at Goldstone) has an 80 kW transmitter installed. There is also a separate task underway

Parameter	Requirement	Measured
G/T 90% weather		
S-Band 6-deg elevation	>=40.2 dB/K	40.5
S-Band zenith	>=40.5 dB/K	41
X-Band 6-deg elevation	>=50.1 dB/K	56.6
X-Band zenith	>=53.4 dB/K	57.1
Ka-Band 6-deg elevation	>=51.5 dB/K	63.7
Ka-Band zenith	>=60.7 dB/K	67
Antenna-microwave temperature - (TAMW), vacuum (zenith)		
S-Band	≤24.4 K (zenith)	20.7
X-Band	≤18.5 K (zenith)	14.1
Ka-Band	≤ 21 K (zenith)	13.5
Antenna gain change vs. elevation		
S-Band	≤ 0.25 dB	0.2
X Band	≤ 0.25 dB	0.15
Ka Band	≤ 1.0 dB	0.87
Antenna gain measurement accuracy		
S-Band	≤ 0.25 dB	0.25
X Band	≤ 0.3 dB	0.25
Ka Band	≤ 0.4 dB	0.25
Antenna Gain Stability (over 20 min.)	<0.1 dB	0.1
Antenna pointing error		
Closed Loop		
S-Band (conscan)	≤ 0.1 dB (≤ 20.0 mdeg MRE)	N/A
X-Band (conscan)	≤ 0.1 dB (≤ 6.0 mdeg MRE)	3.2 mdeg
Ka-Band (monopulse)	≤ 0.1 dB (≤ 1.2 mdeg MRE)	1.0 mdeg
Blind Pointing		
S-Band	≤ 0.1 dB (< 20.0 mdeg MRE)	10 mdeg
X-Band	≤ 0.1 dB (< 6.0 mdeg MRE)	5.8 mdeg
Ka-Band	≤ 0.8 dB (< 4.0 mdeg MRE)	3.4 mdeg
Amplitude Stability (combined U/L, D/L)		
S-S (1000 s)	0.2 dB	0.1
X-X (1000 s)	0.2 dB	0.15
Telemetry Time-tagging Accuracy	3.5 usec	3 usec
System loss, (demodulation/decoding)		
Low Rate (10 bps, r1/2, RS, 0 dB SSNR)	0.25 dB	0.25
Mid Rate (100 kbps, r 1/6, -6 dB SSNR)	0.25 dB	0.25
High Rate (13 Mbps, r 1/2, 0 dB SSNR)	0.25 dB	0.25
Transmitter noise effects: SNT degradation (Kelvin)		
S-Band	< 1 dB	<0.1
X-Band	< 1 dB	<0.1 dB
Ka-Band	< 0.5 dB	<0.1 dB
Phase stability (Allen dev.)		
SS-Band 1000 sec	$<7.7 \times 10^{-15}$	7.5×10^{-16}
X-X-Band 1000 sec	$\leq 5 \times 10^{-15}$	1.5×10^{-15}
X-Ka-Band 1000 sec	$\leq 2.4 \times 10^{-15}$	7×10^{-16}
Phase Noise dBc/Hz		
S-S-Band 1 Hz	-63	-70
X-X-Band 1 Hz	-63	-75
X-Ka-Band 1 Hz	-50	-56
Ranging Measurement meters, 1-sigma	1.0	0.30

Table 1. DSS-36 Compliance Matrix

to deliver the Ka-26 GHz downlink capability to a second BWG antenna at each complex.

An earlier task delivered the Ka-26 GHz equipment to one antenna per complex in 2008-2009 [3]. All of the BWG antennas are required to support radio science missions, which determine the stringent requirements for system stability (phase and amplitude) and spectral purity. The compliance table with the principle system requirements and resulting measurements for DSS-36 is shown in Table 1.

3. Measurement and calibration techniques

3.1 Electronics subsystem and system tests

A DSN beam waveguide antenna consists of several different subsystems, as shown in the block diagram for the X/Ka equipment in Fig. 3. For any new antenna, some new equipment is added to the Signal Processing Center (SPC), shown on the right-hand side of the block diagram. All of the connections to the antenna pedestal area are then made via fiber optic links (both multi-mode and single-mode). The various subsystems are installed independently, followed by assembly-level hardware checkout tests. These are followed by formal acceptance tests (AT) for each subsystem. The ATs are run according to released procedures which are used whenever new hardware or subsystem software is delivered to the DSN. Alignment of system gain is done at this stage also, to optimize the system dynamic range. This is done by measuring system linearity and follow-on temperature, and then adjusting the front-end and back-end gain to achieve the best compromise. An example of the independent assemblies is the separate feed/LNA assemblies for S-band and X/Ka-band (shown in Fig. 4 and 5 respectively). The majority of the other RF electronics assemblies (upconverters, downconverters, etc.) are mounted on uni-strut frames in the antenna pedestal (Fig. 6).

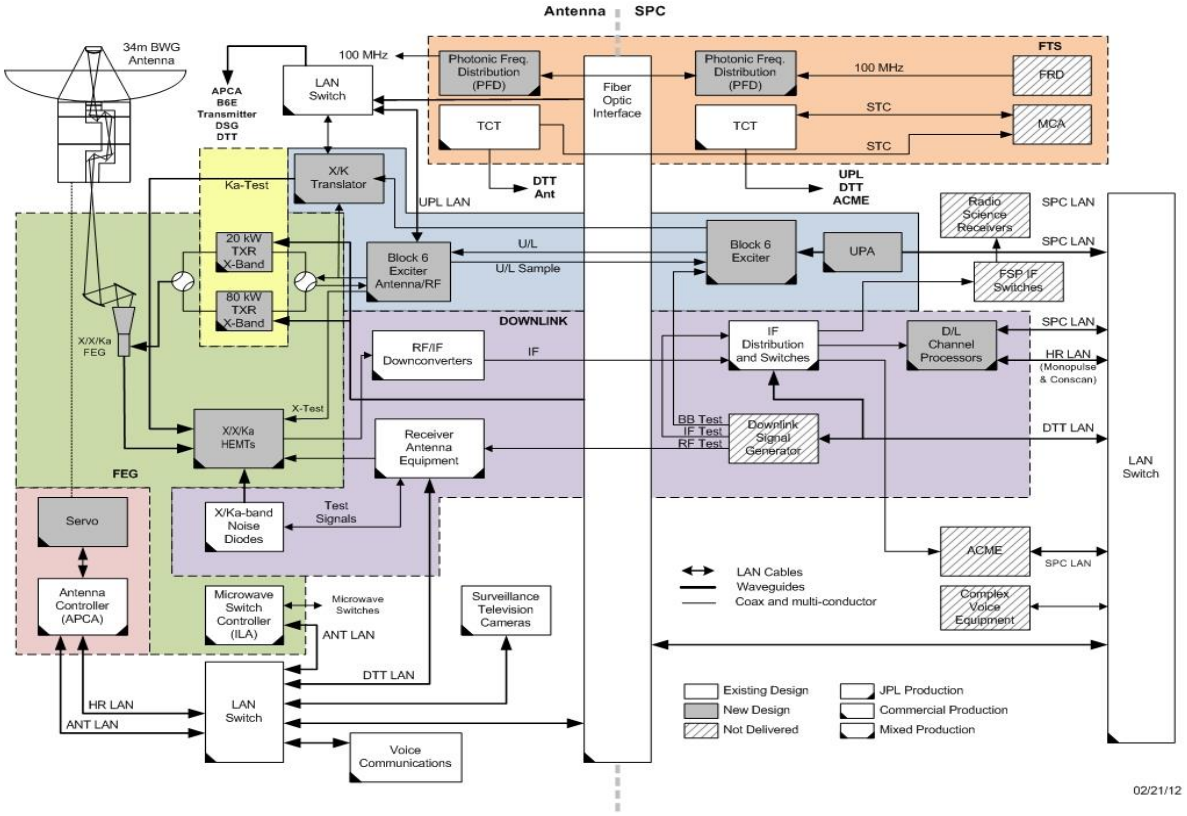

Fig. 3 BWG antenna block diagram for X/X/Ka-band

Fig. 4 S-band feed and cryostat assembly

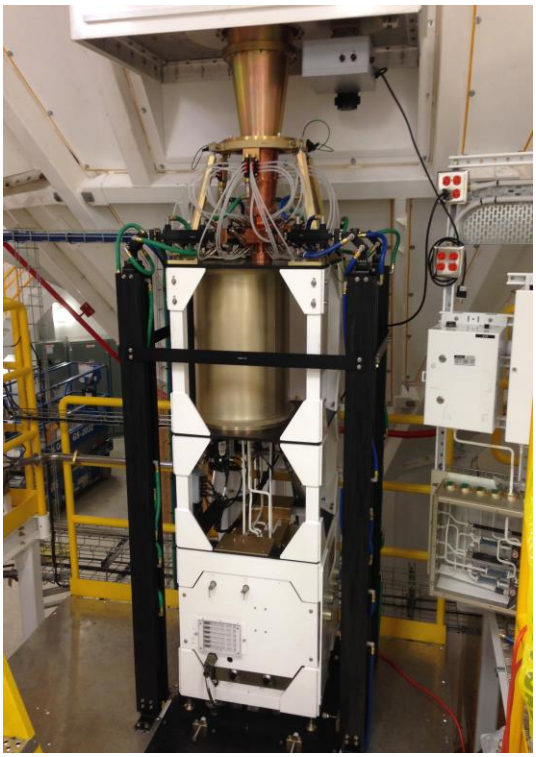

Fig. 5 X/Ka-band feed and cryostat assembly

Fig. 6 RF electronics adjacent to BWG shroud

After completion of the AT testing, a standard set of system performance tests (SPTs) is run. These tests include a comprehensive set of procedures to verify tracking, telemetry and command (TT&C) performance, as well as compliance with radio science requirements. A summary of the SPT test results is shown in the compliance table for the DSS-36 antenna in Table 1.

3.2 Antenna calibration and optimization

Two major RF assemblies were utilized for the calibration and performance optimization of the antennas. These are the Antenna Holography Measurement Group (AHMG), and the Antenna Calibration & Measurement Equipment (ACME) assembly [4]. The AHMG utilizes a coherent amplitude and phase receiver operating at the full range of the Ku-Band frequency range, of commercial geostationary satellites, between 10.7 to 12.9 GHz. The ACME utilizes non-coherent detection of radio sources, such that it can detect signals at all of the operational frequency bands and full bandwidth of the DSN operational antennas. These include S, X, Ka-26, and Ka-32 GHz-band frequencies as described in section 2 of this article. ACME operates in both total power radiometry (TPR) and noise adding radiometry (NAR) modes [4].

The advantage of the AHMG system is that it takes advantage of a stationary and strong signal source provided by the satellite, which is in the antenna far-field region. The typical satellite's signal source strength is 11-dBW. The range to the OPTUS D-1 satellite, used in Australia, for the calibration of the two antennas described in this article, is approximately 35,780-km, while the beacon frequency used was 12.749-GHz. Figure 7 shows the AHMG high-level diagram.

The AHMG Ku-Band feed is first installed at the antenna in its F1 focus location and used to align the antenna subreflector and set the main reflector dish panels. An initial photogrammetry technique was also used in an earlier stage, to set the main reflector panels, achieving a normal rms error of 0.266-mm. Upon completion of the holography calibration from the F1 focus, the front-end package was moved to the f3 focus. From the F3 focus measurements, the integrity of the mechanical alignment of the 5 major BWG mirrors can be determined, and their contribution to the antenna rms from this operating focus position. Figures 8 and 9, show the installation of the AHMG front-end packages in the F1 and F3 foci of the DSS-36 antenna.

After the conclusion of the AHMG calibration phase, the calibration and performance characterization of the antennas is done in their operational frequency bands and in both right-hand-circular (RCP) and left-hand-circular (LCP) polarizations. During this calibration and measurement phase the antenna noise-temperature was measured and determined, including system linearity. The sub reflector was also further focused, relative to the antenna F3 focus, and over the entire operational elevation angle range of the antenna (90 to 6-degrees). The antenna 4th order [4, chapter 7] pointing model data gathering and derivations was also done for each frequency band. Tipping data curves were measured and corrected for atmospheric contribution, and antenna efficiency in all operational frequency bands and over the full elevation operational range of the antennas was determined. The antenna efficiency and all other measurement parameters via ACME are currently computed and referenced to the antenna feed horn aperture. When the atmospheric noise-temperature contribution correction is being corrected out of the data, the resulted quantity is referred to antenna and microwave noise-temperature (Tamw, as would have been measured in vacuum). From these

measurements, the antenna's G/T performance is being computed.

DSS-35 and -36 were also retrofitted with a new assembly: Antenna Transmitter Mask Controller (ATMC). This assembly replaced the older mechanical version, which was limited to a few actuators placed along the antenna azimuth track and elevation gear. These switches would then control when the high-power transmitter would turn off and on relative to the surrounding terrain in order to meet ITU radiation standards. The new ATMC allows for computer controlled determination of the transmit and receive horizon masks with resolutions of 0.1-degrees. In determining the mask for each antenna, radiometric techniques utilizing ACME were deployed to derive these high-resolution masks [5], and radiometric criteria were used for their derivation. These were, 2.5-kelvin rise in Tamw, as a threshold for the transmitter mask, and 50-kelvin rise in Tamw, for the receive mask.

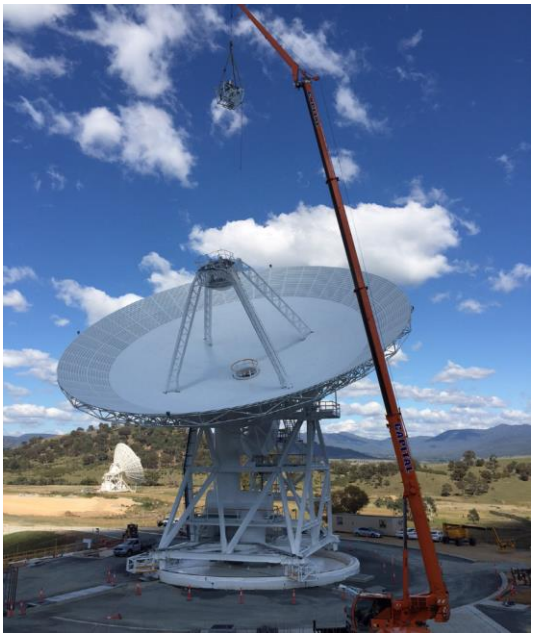

Figure 8. Installation of AHMG Front-End at F1

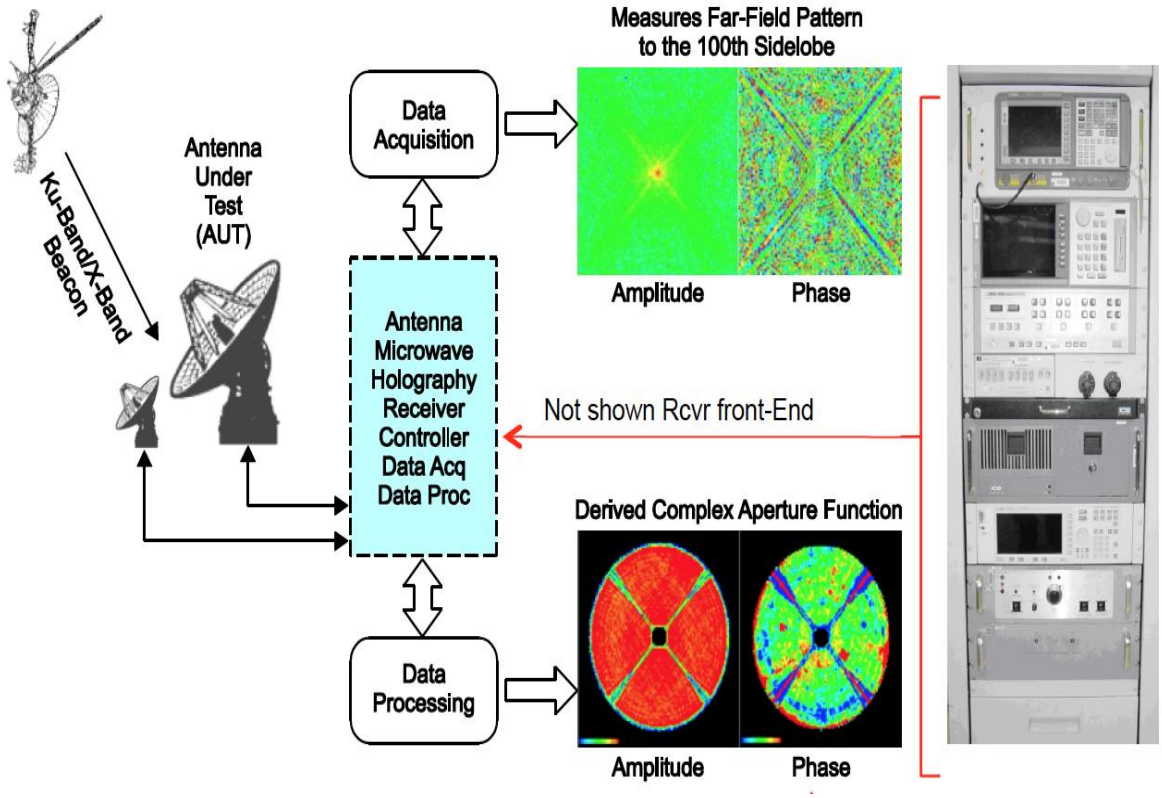

Figure 7. AHMG High-Level Diagram

Figure 9. AHMG Front-End installed at F3

3.3 Shadow tracks and project interface tests (PITs)

Following successful completion of the SPT phase of testing, the antenna is considered to be ready for actual spacecraft tracking. The test track phase is normally done in two segments: shadow tracks and PITs. For a shadow track, the new antenna is used to track a spacecraft in downlink-only mode, in parallel with an operational antenna at the same complex. The purpose of this test is to compare overall performance for system noise temperature (SNT) and carrier-to-noise ratio (Pc/No) for the downlink carrier.

For a new DSN antenna, PITs are run with many different spacecraft, to verify as many of the TT&C functions as possible. For these tests, command data is flowed to the DSN complex from the project Mission Operations Center (MOC), and telemetry from the downlink is flowed back to the MOC. Ranging and Doppler data is analyzed locally by the JPL Navigation team to verify consistency with data from operational antennas. Any of the antennas at a DSN complex can be arrayed to improve the downlink SNR, and this configuration was verified with an array track for Voyager 2 (VGR2) using both DSS-35 and -36. Conversely, a single antenna can be used to track multiple downlinks within the same beam, and this occurs regularly for the Mars missions. This so-called Multiple Spacecraft per Antenna (MSPA) mode was also verified for both DSS-35 and -36. The list of spacecraft and frequency bands for which PITs were run with DSS-36 is given in Table 2.

PITs Run with DSS-36, July-August, 2016

S/C	Band	Doppler	RNG	CMD	TLM
MVN	X	1W	NO	YES	YES
VGR2	X	1W	NO	NO	NO
CAS	X, Ka	2W	YES	YES	YES
M010	X	1W, 2W	YES	YES	YES
MEX	X	1W, 2W	YES	YES	YES
MRO	X	1W, 2W	NO	YES	YES
STA	X	2W	YES	YES	YES
NHPC	X	1W, 3W	YES	YES	YES
GTL	S	1W	NO	YES	YES
ACE	S	2W	YES	YES	YES
LRO	S	2W	YES	YES	YES
MMS1-4	S	2W	NO	YES	YES
MSL	X	2W	NO	YES	YES
VGR1	X	1W	NO	YES	NO
DAWN	X	2W	YES	NO	YES
JNO	X, Ka	2W	YES	NO	YES
CHDR	S	2W	YES	YES	YES
WIND	S	2W	YES	YES	YES
SOHO	S	2W	NO	YES	YES
STF	X	2W, 3W	NO	YES	NO

Table 2. Mission set for DSS-36 PITs

The DSN antennas are also occasionally used for Delta Differential One-way Ranging (DDOR). This tracking mode is used for precision angular determination, to supplement the ranging measurements that are regularly done using sequential or pseudo noise (PN) ranging with a single antenna [6]. For the DDOR measurements, two antennas, from different

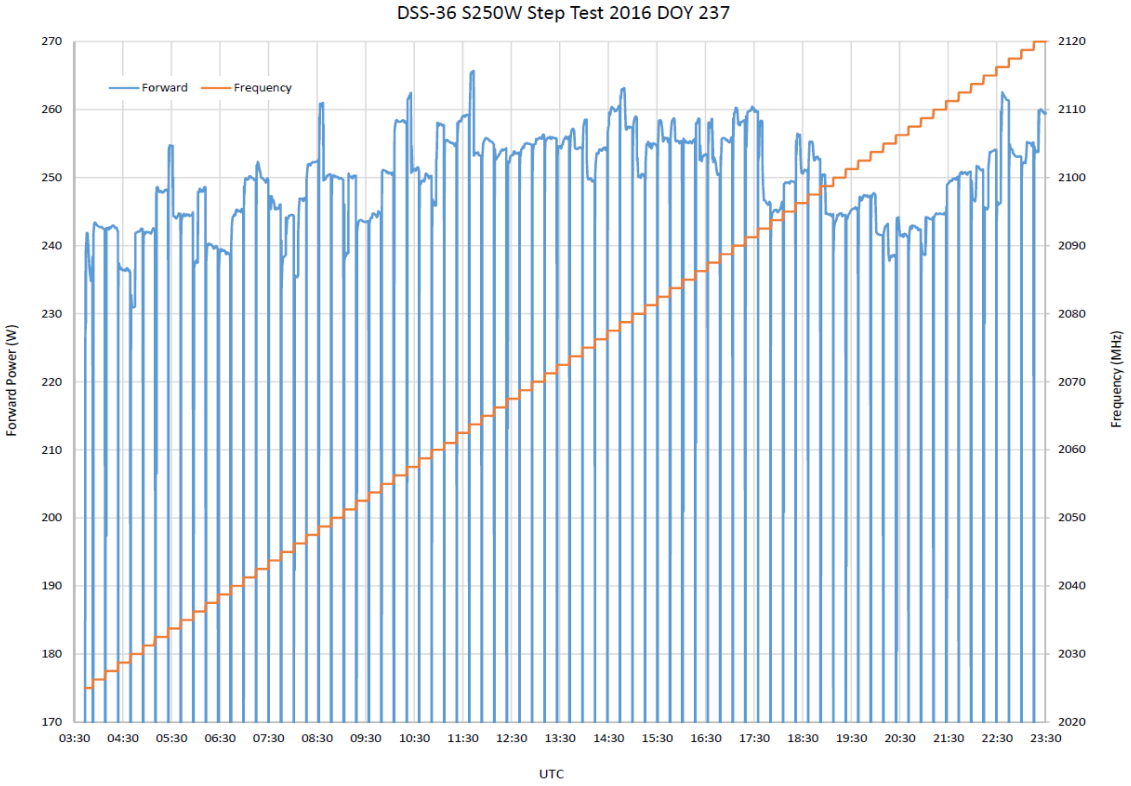

Fig. 10 S-band transmitter step test

DSN complexes, are used simultaneously to track a single spacecraft with a wide baseline.

Finally, a new antenna needs to have Very Long Baseline Interferometry (VLBI) measurements performed, to determine its precise location on the earth. This is done by tracking a known radio star simultaneously with an existing antenna, either at the same or a different complex.

4.0 Results

4.1 Electronics subsystem and system tests

As part of the subsystem acceptance tests, the frequency response for the uplink and downlink equipment is measured independently. For the feed/LNA combination, the noise temperature vs. frequency is measured for all bands (S, X and Ka for DSS-36). For the exciter/transmitter subsystem, the frequency response is characterized by running a "step test" across the band. In this test, the exciter frequency is varied in 1 MHz steps across the 95 MHz band while the transmitter output is measured with a power meter. For each step, the normal calibration routine is run to set the output to the target power, within approximately +/- 5%. A typical step test run at DSS-36 with the S-band 250 W transmitter is shown in Fig. 10.

Many of the SPT tests are run with the uplink and downlink subsystems together, using the test translator to do a test signal turn-around. This includes translation from one uplink band to a different downlink band. The most commonly used translations are S-S, X-X and X-Ka. However, the other combinations (S-X, X-S) are tested during the commissioning phase of a new antenna. An example of X-Ka system phase stability (Allan deviation) and phase noise is shown in Fig. 11 and Fig. 12.

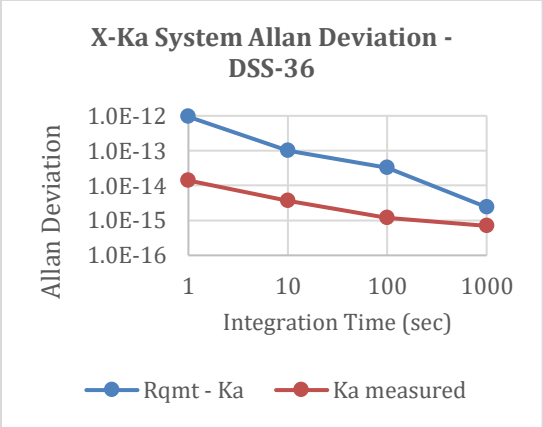

Fig. 11 X-Ka system Allan deviation

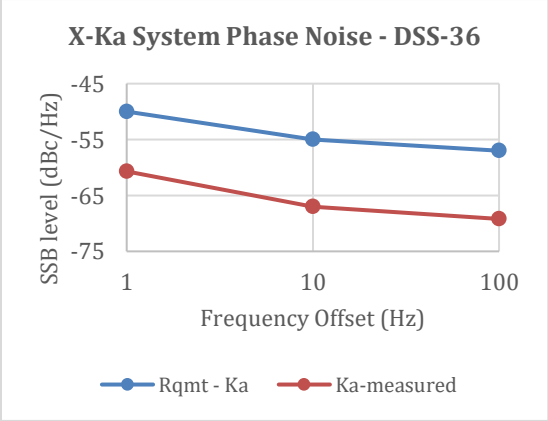

Fig. 12 X-Ka system phase noise

4.2 Antenna calibration and optimization

Figure 13 shows the DSS-35 far-field pattern as derived from observing OPTUS D-1 at 12.749-GHz. The high fidelity in these measurements enable high accuracy, high precision panel settings and other parametersderivations.

Figure 14 Shows a far-field elevation cut of DSS-35 which was measured by the AHMG, showing the first side lobes below 17-dB of the main beam as expected for this dual-shaped Cassegrain reflector antenna. While figure 15 shows the derived antenna amplitude aperture illumination confirming the uniform illumination design for this antenna. This design achieves higher aperture efficiency as needed for deep space telecommunication, in comparison for the traditional Cassegrain tapered illumination which is being used primarily in radio astronomy and which achieves better beam efficiency.

Figure 16 shows the DSS-36 normal root mean square (rms) error of the combined surfaces of the subreflector and main dish before and after applying holography-derived panel settings, imaged from the F1 Cassegrain focus. The rms error was reduced from 0.266 to 0.192-mm rms both at a resolution of 33-cm.

This improvement in panel alignment (alone) corresponds to 4% increase in efficiency at Ka-Band, or +0.27-dB, and enable an antenna aperture efficiency at Ka-Band of 66%. In comparison, the final rms surface of DSS-35 was 0.202-mm.

Figure 17 shows the ultimate possible rms error that could be achieved (time permitting for additional panel alignments), and which is limited by the rms of the individual panels, subreflector, and each of the 7 BWG mirrors. Derivation are made for these ultimate performances from F1 and F3 foci with the results of 127 and 198-micron for the normal surface. These can be compared with the theoretical computations based on manufacturer records of 121 and 196-micron. The resolution in these images is 10-micron and they reveal the imperfections in the manufacturing of the individual panels and mirrors.

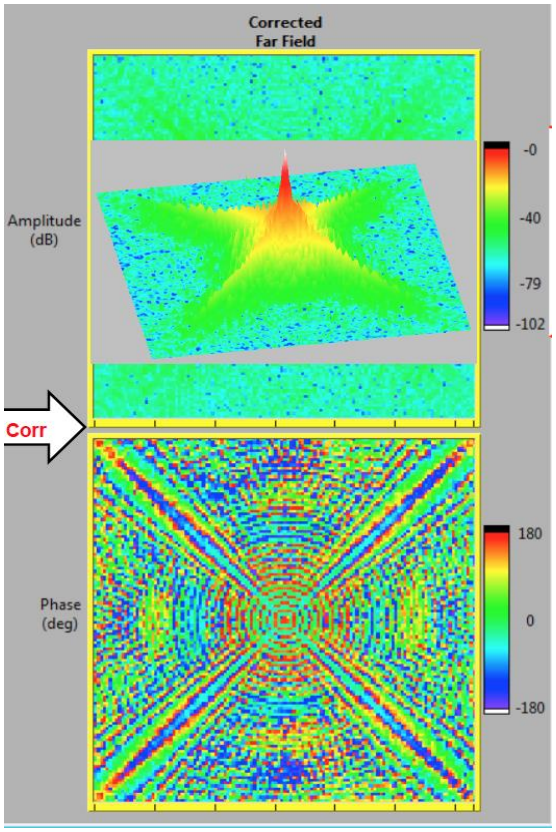

Fig. 13 Holography Measurement of DSS-35 far-Filed pattern over a 2.2 x 2.2-degrees directional cosine window, and with 102-dB dynamic range. OPTUS D-1 at 12.749-GHz

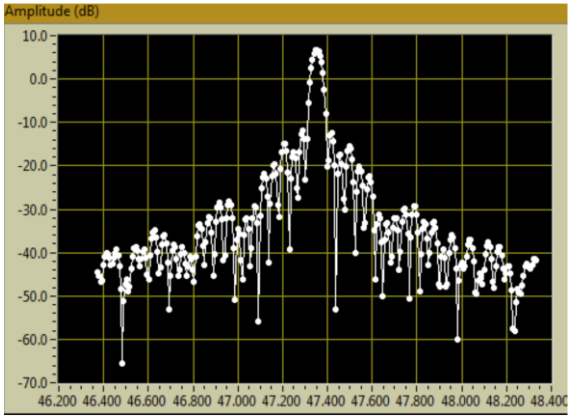

Fig. 14 DSS-35 Far-Filed Elevation Cut Patterns

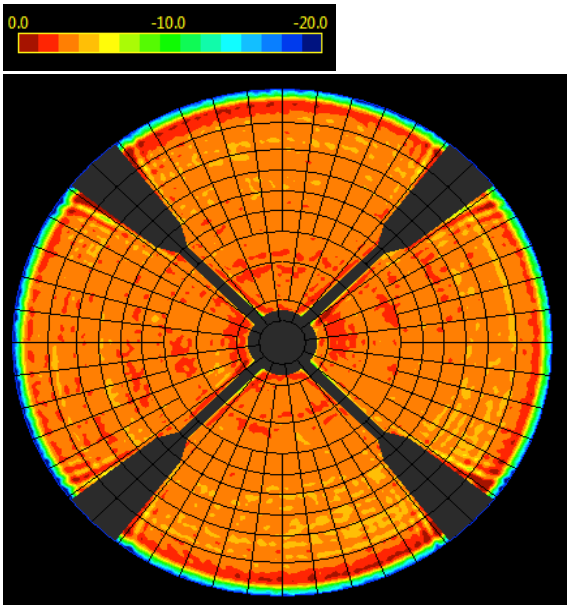

Fig. 15 DSS-36 Aperture Amplitude Illumination

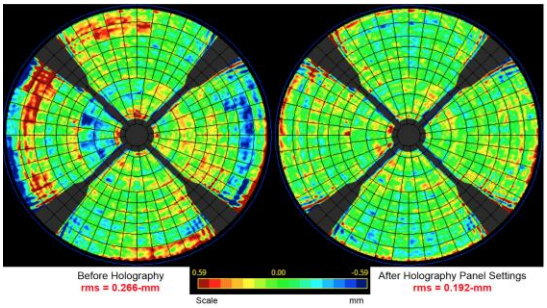

Fig. 16 Antenna Normal rms error after photogrammetry (left) and after holography (right)

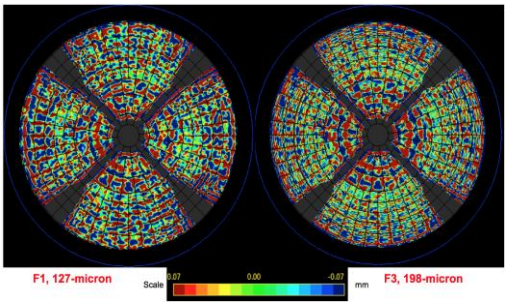

Fig. 17 Theoretical minimum surface rms error

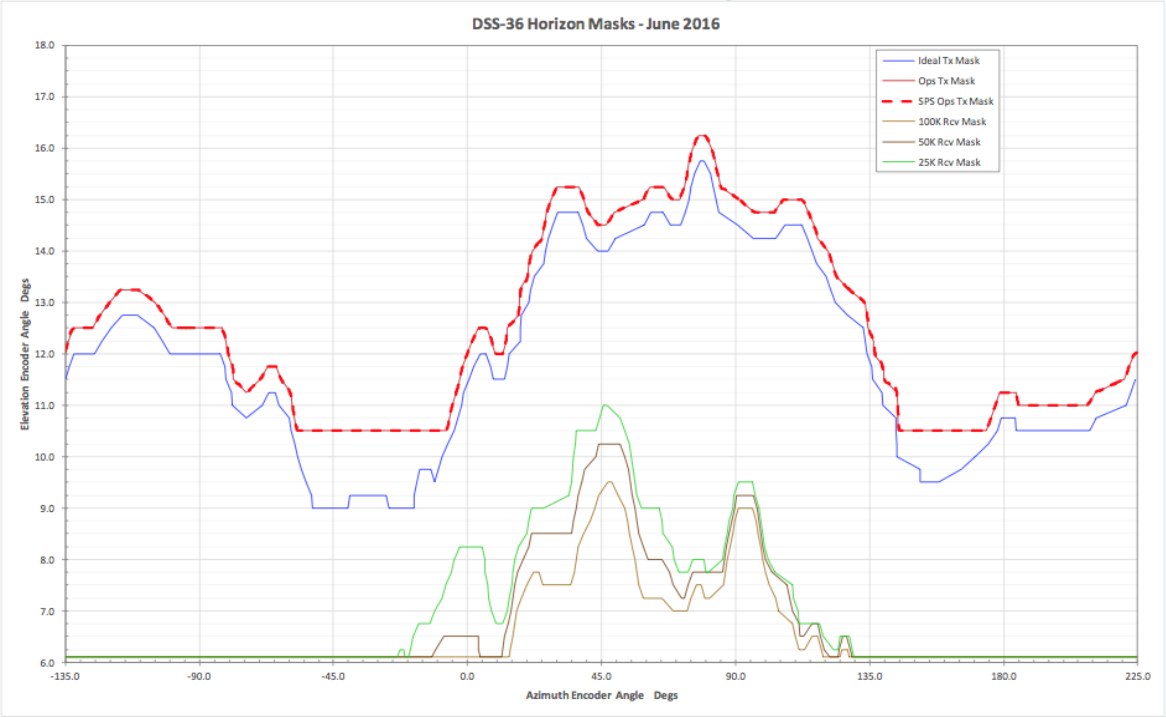

Fig. 19 Derived DSS-36 transmit and receive masks for ATMC

Upon completion of the holography calibration work, we switch to the radiometry calibration, utilizing the installed front-end feeds, LNA,s, and down-converters of the operational antenna.

Table 3. shows the ACME derived parameters for DSS-36 noise temperatures, linearity, and Tamw, along with the requirements.

FREQUENCY	CONFIGURATION	POLARIZATION	LINEARITY (%)	T-AMW, ZENITH, ACME (kelvin)	Req. AMW FRD (kelvin)
32.0 GHz	X/X/Ka	RCP	-0.97	13.5	<=18.7
32.0 GHz	X/X/Ka	LCP	-0.07	12.5	<=18.7
8.450 GHz	X/X/Ka	RCP	-0.63	12.73	<=18.5
8.450 GHz	X/X/Ka	LCP	-0.12	14.062	<=18.5
2.295 GHz	S –low noise	RCP	0.43	20.74	<=24.4
2.295 GHz	S/X - Diplexer	RCP	0.43	36.3	<=40.0

Table 3. DSS-36 Noise Temperature for the various configurations.

The critical results for the antenna efficiency at Ka-Band (32-GHz) are shown in figure 18 for DSS-36. The antenna peak aperture efficiency is 66%, achieved near the rigging angle of 47-degrees elevation, where the panel setting took place (as a result of the combination of the station and satellite locations). The rigging angle is slightly biased towards the higher elevation angles, and the more complex atmospheric corrections are at the lower angles. As a result, the approximate gain roll-off for DSS-36 with elevation is 0.87-dB.

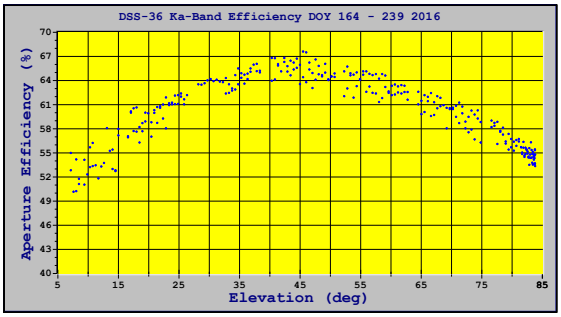

Fig. 18 DSS-36 Aperture Efficiency at Ka-Band (32-GHz) RCP

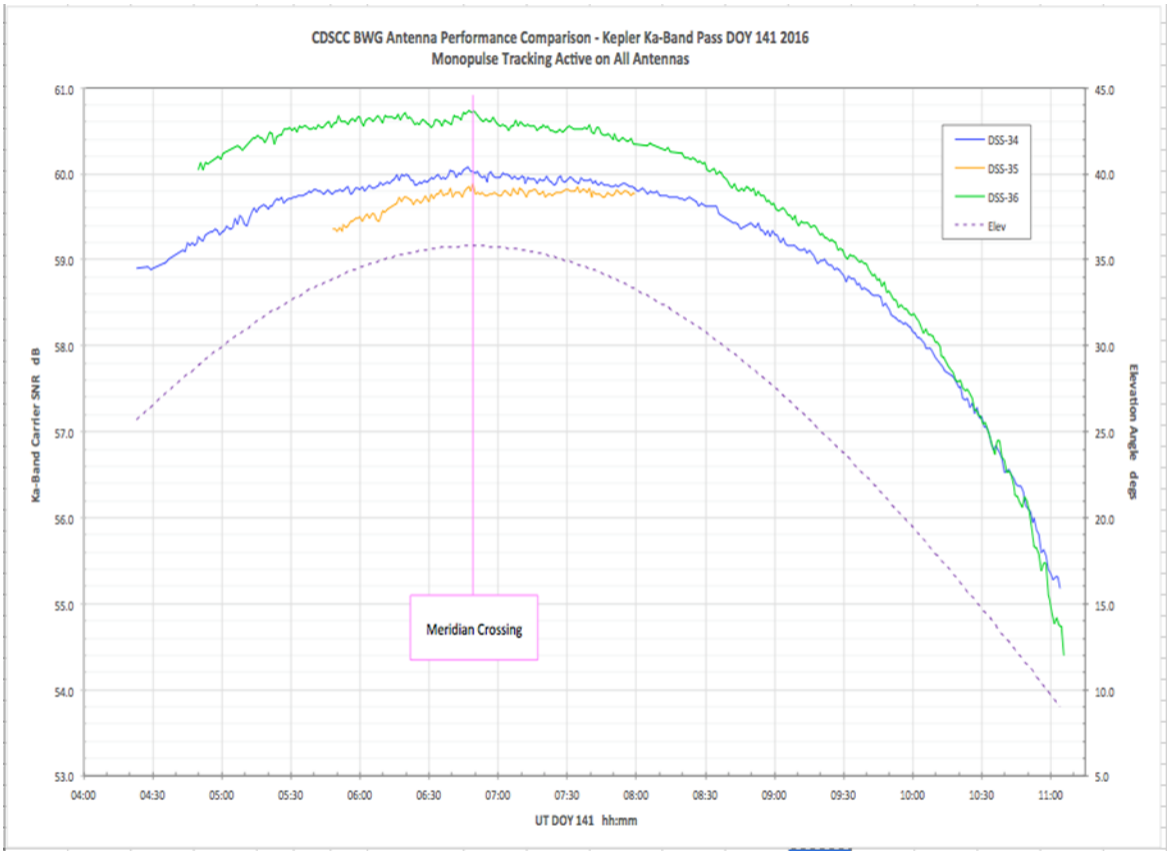

Fig. 20 Ka-band shadow track for Kepler with DSS-34, -35 and-36: Pc/No vs time

The Horizon mask derived during this stage is presented in figure 19. It shows the both the transmit and receive masks for DSS-36 based on the criteria's described in section 3.2

4.3 Shadow tracks and PITs

Shadow track results for the newest antenna, DSS-36, vs the other BWG antennas in Canberra are shown in Fig. 20 (Ka-band). This example shows the results from a track with Kepler at Ka-band, where the new DSS-36 antenna was run in shadow mode to the operational DSS-34 and -35 antennas. The plot shows a comparison of the carrier-to-noise ratio (Pc/No) for the three antennas over the 7-hour duration of the track. The new antenna is seen to be slightly better (by about 0.7 db) in G/T for most elevations of the pass.

This was expected, given that the efficiency of DSS-36 at Ka-band is higher than the other two antennas. For the PITs, downlink performance of the new antenna is verified by analysis of telemetry at the MOC. Commanding is tested by sending no-op command logical transmission units (CLTUs) to the spacecraft, and verifying that they are correctly received on-board. Tracking with the new antenna is confirmed by analysis of parameters such as Doppler residual and ranging residual, as shown in Fig. 21 and Fig. 22.

For confirmation of correct DDOR tracking performance, tests were run using the MRO spacecraft, and three different antennas. In this case, the common antenna was DSS-26 (at Goldstone), the second existing antenna was DSS-43 (in Canberra) and the new antenna was DS-36. The spacecraft was then tracked from all 3 antennas, and the data processed to produce

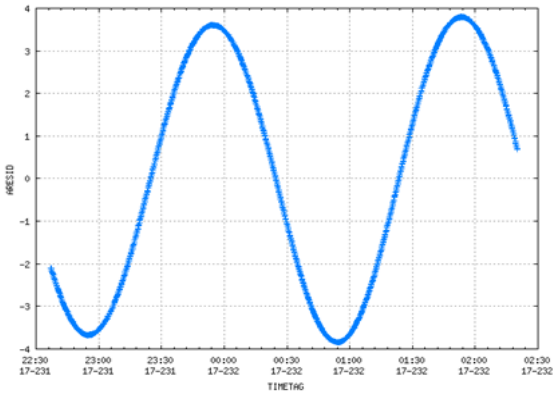

Fig. 21 2-way Doppler residuals (Hz) for Mars Odyssey PIT with DSS-35

correlated results for 2 different baselines: 26/43 and 26/36. Delay residuals for the two different baselines are shown in Fig. 23 and Fig. 24. The proper functioning of the new antenna (36) is confirmed by the similar results in the two plots.

For the antenna location determination, VLBI tracks were run for each "new" antenna, together with the existing DSS-34. These tracks were run for both X and Ka-band, over the full range of azimuth and elevation. An example of a successful X-band correlation fringe is shown in Fig. 25. The precise location of the new antenna was analyzed to be accurate to +/-1 mm.

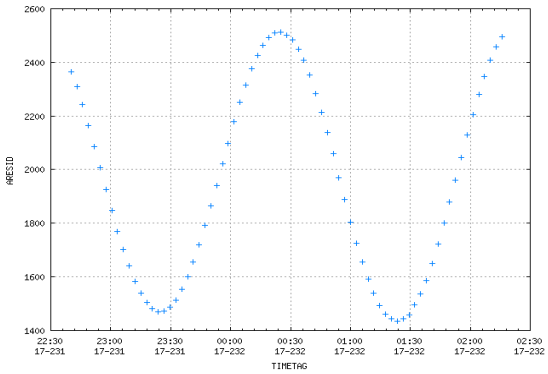

Fig. 22 Sequential range residuals (RU) for Mars Odyssey PIT with DSS-35

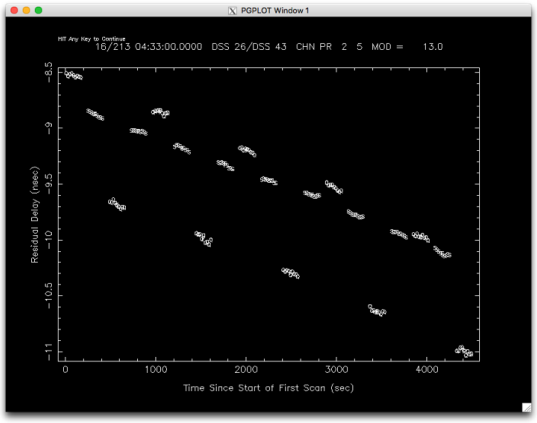

Fig. 23 DDOR Delay Residuals Baseline (DSS-26/43 with MRO)

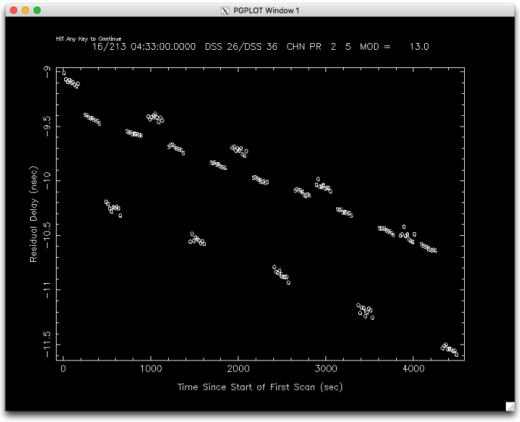

Fig. 24 DDOR Delay Residuals (DSS-26/36 with MRO)

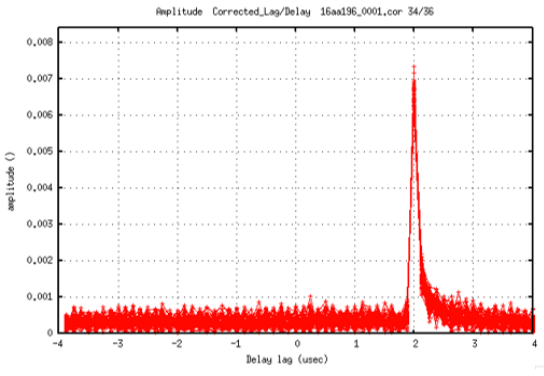

Fig. 25 VLBI X-band fringe, DSS-36 with -34

5.0 Conclusion

The DAEP project is providing a major addition to the capability of the DSN, allowing the network to support an increasing number of missions at S, X and Ka-bands. Following a comprehensive series of calibrations and tests for both the electronics and the antenna, the first of the new BWG antennas in Canberra (DSS-35) was completed in 2014 and the second (DSS-36) became operational in 2016. Looking to the future, the design updates that were done under the DAEP project will allow for future upgrades such as the addition of an 80 kW X-band transmitter, Ka-26 GHz downlink, uplink arraying and Ka-band (34 GHz) uplink.

The next two DSN antennas, at the Madrid complex, are planned to be operational in 2020.

Acknowledgement

The implementation described in this paper was carried out by the Jet Propulsion Laboratory, California Institute of Technology, at the DSN complex in Canberra, Australia, under a contract with the National Aeronautics and Space Administration. The authors would like to thank the DAEP project managers, Miguel Marina and Bradford Arnold, for funding and guidance throughout the task. The authors would also like to thank all of the engineers at both JPL and Harris Corporation, who supported the integration and test. In addition, the authors would also like to especially thank the engineers at the Commonwealth Scientific and Industrial Research Organization (CSIRO) who contributed to the electronics and antenna testing and calibration: Graham Baines, Kevin Boroczky, Nigel Chauncy, Kevin Piechowski, Tim Olin, Paul Richter and Ashish Soni.

References

[1] R. Cesarone, D. Abraham and L. Deutsch, "Prospects for a Next-Generation Deep Space Network", Proceedings of the IEEE, Vol. 95, No. 10, October 2007.

[2] R. LaBelle and C. Buu, "Uplink and Downlink Electronics Upgrades for the NASA Deep Space Network Aperture Enhancement Project (DAEP)", Proceedings of the SpaceOps 2014 Conference, May 5-9, 2014.

[3] R. LaBelle, D. Rochblatt, "Ka-band High-Rate Telemetry System Upgrade for the NASA Deep Space Network", Acta Astronautica, Vol. 70, January, 2012, doi:10.1016/j.actaastro.2011.07.023.

[4] M. Reid editor, Low-Noise Systems in the Deep Space Network (JPL Deep-Space Communications and Navigation Series), Chapters 7 and 8 (D. Rochblatt). September 29, 2008.

[5] David Rochblatt, Graham Baines, Tim Olin, Manuel Vazquez "Holographic Measurements and Performance of the NASA-JPL-DSN new 34-m BWG Antennas", NRAO Metrology and Control of Large Telescopes, September 20 - 24, 2016.

[6] G. Lanyi, D. Bagri and J. Border, "Angular Position Determination of Spacecraft by Radio Interferometry", Proceedings of the IEEE, Vol. 95, No. 11, November 2007.